Compact Multistage Plasma-Based Accelerator Design for Correlated Energy Spread Compensation

A. Ferran Pousa,[1,2,*] A. Martinez de la Ossa,[1] R. Brinkmann,[1] and R. W. Assmann[1]

[1] *Deutsches Elektronen-Synchrotron DESY, 22607 Hamburg, Germany*
[2] *Institut für Experimentalphysik, Universität Hamburg, 22761 Hamburg, Germany*

(Dated: July 26, 2019)

The extreme electromagnetic fields sustained by plasma-based accelerators could drastically reduce the size and cost of future accelerator facilities. However, they are also an inherent source of correlated energy spread in the produced beams, which severely limits the usability of these devices. We propose here to split the acceleration process into two plasma stages joined by a magnetic chicane in which the energy correlation induced in the first stage is inverted such that it can be naturally compensated in the second. Simulations of a particular 1.5-m-long setup show that 5.5 GeV beams with relative energy spreads of 1.2×10^{-3} (total) and 2.8×10^{-4} (slice) could be achieved while preserving a sub-micron emittance. This is at least one order of magnitude below the current state-of-the-art and would enable applications such as compact free-electron lasers.

Plasma-based accelerators (PBAs), driven either by charged particle beams [plasma wakefield accelerator (PWFA)[1]] or intense laser pulses [laser wakefield accelerator (LWFA)[2]], are able to sustain accelerating gradients in excess of 100 GeV/m [3]. These extreme gradients are orders of magnitude higher than those achievable with radio-frequency technology and offer a path towards miniaturized particle accelerators with groundbreaking applications in science, industry and medicine [4].

Steady progress over the past decades has led to the successful demonstration of electron bunches with multi-GeV energy [5–9], micron-level emittance [10, 11] and kiloampere current [12, 13]. However, the high amplitude and short wavelength ($\sim$ 100 µm) of the wakefields naturally imprint a longitudinal energy correlation (or chirp) along the accelerated (witness) bunch, leading to a large relative energy spread typically on the 1-10 % range [14]. This is a long-standing issue for PBAs which can, in addition, lead to a large emittance growth [15, 16]. Achieving a small emittance and energy spread is however essential for applications such as in high-energy physics [17] or, in particular, for free-electron lasers (FELs) [18–22], which demand an energy spread $\lesssim 0.1\%$ [23].

Solving this issue is therefore key for demonstrating the usability of PBAs. A well known concept for mitigating the correlated energy spread is that of beam loading [24–26], in which the witness bunch itself is used to flatten the slope of the accelerating fields. This, however, relies on a very precise shaping of the current profile and has yet to be demonstrated with the desired performance. Furthermore, since the optimal profile depends on the wakefield structure, a certain energy spread will always develop in LWFAs, where the wakefield experienced by the bunch will change due to the laser evolution [27, 28] as well as dephasing [29]. Alternative ideas have also been proposed in order to achieve, in average, a flat accelerating gradient. These include modulating [30] or tailoring [31] the plasma density profile as well as injecting a secondary bunch [32], but they show limited success or remain to be experimentally realized. Other dechirping techniques based on beam-induced wakefields have been proposed [33] and even demonstrated experimentally [34–38], although not for the extreme chirps imprinted by PBAs.

We propose here a novel concept for compensating for the correlated energy spread in PBAs which takes advantage of the naturally occurring energy chirp. In this scheme, as illustrated in Fig. 1, it is proposed to split the acceleration process into two identical plasma stages joined by a magnetic chicane. This chicane inverts the longitudinal energy correlation of the bunch generated in the first plasma stage such that it can be compensated in the second. Numerical simulations with the Particle-in-Cell (PIC) code FBPIC [39] as well as the tracking codes ASTRA [40] and CSRtrack [41] show that multi-GeV beams with unprecedented energy spread could be obtained with this method. These promising results show that the presented concept could enable innovative applications such as the realization of compact FELs.

In order to introduce this concept, the blowout regime [42–44] of plasma acceleration will be considered. In this case the laser or beam driver is able to expel all background plasma electrons, leaving behind an ion cavity with a uniform focusing gradient, $K = (m/2ec)\omega_p^2$, and an approximately constant longitudinal electric field slope, $E_z' \equiv \partial_z E_z \simeq (m/2e)\omega_p^2$, along most of the accelerating phase. Here $\omega_p = \sqrt{n_p e^2/m\epsilon_0}$ is the plasma frequency, e and m the electron charge and mass, ϵ_0 the vacuum permittivity and n_p the unperturbed plasma density. In order to describe the position and energy of the particles along the accelerator it is also useful to introduce the speed-of-light coordinate, $\xi = z - ct$, as well as the relativistic Lorentz factor, $\gamma = 1/\sqrt{1-(\boldsymbol{v}/c)^2}$, where t is the time and $\boldsymbol{v}$ and z are, respectively, the particle velocity and longitudinal position in the laboratory frame. Within the generated cavity, electrons perform transverse oscillations (known as betatron motion) with a frequency $\omega_\beta(t) = \sqrt{eK/m\gamma(t)}$, while their energy

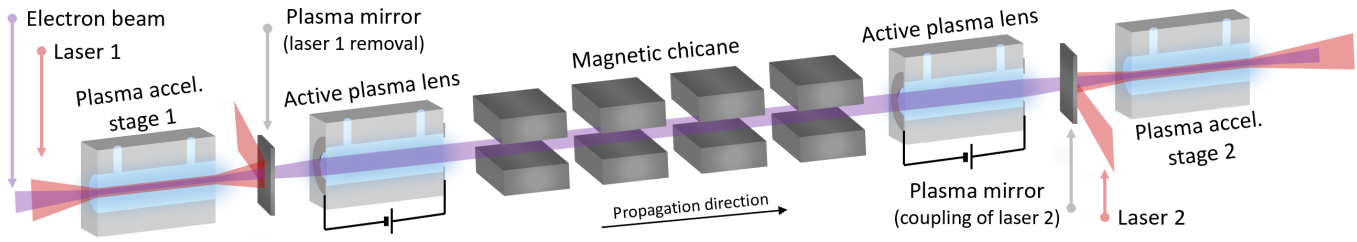

FIG. 1. Schematic view of a possible implementation of the energy chirp compensation concept.

evolves as $\gamma(t) = \gamma_0 - (e/mc)E_z t$.

For a particle bunch with average energy $\bar{\gamma}(t) = \langle\gamma(t)\rangle$ centered at $\bar{\xi}$, the longitudinal chirp can be expressed as $\chi(t) = \langle\Delta\xi\Delta\gamma(t)\rangle \,/\, \langle\Delta\xi^2\rangle\, \bar{\gamma}(t)$, where $\Delta\gamma(t) = \gamma(t) - \bar{\gamma}(t)$ and $\Delta\xi = \xi - \bar{\xi}$. A simple expression for the chirp evolution within a plasma stage can be obtained if a constant E'_z is assumed. This yields

$$\chi(t) = \left(\chi_0\bar{\gamma}_0 - \frac{e}{mc}E'_z t\right)\bar{\gamma}(t)^{-1} \,, \tag{1}$$

which tends asymptotically to $\chi = E'_z/E_z$ and where χ_0 and $\bar{\gamma}_0$ are the initial bunch chirp and energy. If the bunch length is $\sigma_z = \sqrt{\langle\Delta\xi^2\rangle}$, this induces a correlated energy spread $\sigma_\gamma^{\rm corr}(t)/\bar{\gamma}(t) = \chi(t)\sigma_z$. In a 2-stage accelerator as in Fig. 1, the accumulated chirp after a first stage of length $L_{p,1}$ for an initially unchirped bunch will be $\chi_1 = -(e/mc^2)E'_{z,1}L_{p,1}/\bar{\gamma}_1$. Therefore, if the longitudinal phase space of the bunch is inverted at this point such that $\hat{\chi}_1 = -(\sigma_{z,1}/\sigma_{z,2})\chi_1$ is obtained, the correlated energy spread could be compensated for in a following stage fulfilling $E'_{z,2}L_{p,2} = (mc^2/e)\hat{\chi}_1\bar{\gamma}_1$. For a symmetric inversion ($\sigma_{z,1} = \sigma_{z,2}$), using two identical plasma stages (same E'_z and L_p) would be the simplest setup.

This longitudinal phase space inversion can be performed with a conventional chicane. As illustrated in Fig. 2, this device is composed by 4 dipole magnets in which particles undergo an energy-dependent trajectory bend. With respect to a hypothetical reference particle with $\gamma = \gamma_{\rm ref}$, those with $\gamma > \gamma_{\rm ref}$ experience less bending and therefore a shorter path length, while the opposite occurs for those with $\gamma < \gamma_{\rm ref}$. Defining $\delta = (\gamma - \gamma_{\rm ref})/\gamma_{\rm ref}$, the path length differences after the chicane, $\Delta\xi_{\rm ch}$, can be expressed with respect to the reference particle as

$$\Delta\xi_{\rm ch}(\delta) = R_{56}\delta + T_{566}\delta^2 + \mathcal{O}(\delta^3) \,, \tag{2}$$

where $T_{566} \simeq -3/2R_{56}$ [45]. To first order, the R_{56} coefficient can be simply determined as $R_{56} = \Delta\xi_{\rm ch}/\delta = \Delta\xi_{\rm ch}/\chi\Delta\xi$ (assuming $\gamma_{\rm ref} = \bar{\gamma}$). From Eq. (2) it can be seen that, for example, maximum bunch compression can be achieved if $\Delta\xi_{\rm ch}$ exactly compensates for the initial offsets with respect to the bunch center, $\Delta\xi$. Similarly, a chirp inversion can be performed if $\Delta\xi_{\rm ch} = 2\Delta\xi$ and, thus, $R_{56} = 2/\chi$.

This technique is therefore ideally suited for bunches dominated by a linear chirp, as is often the case in PBAs,

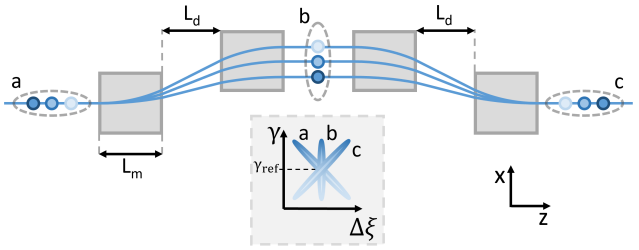

FIG. 2. Working principle of a magnetic chicane with $R_{56} = 2/\chi$. The bunch longitudinal phase space is shown at the chicane entrance (a), middle (b) and exit (c). Darker color implies higher energy.

and thus particularly for the case of weakly beam-loaded wakefields, where a constant E'_z is not perturbed by the bunch, or where the beam-loading effect linearly modifies E_z [26]. When this is not the case, the scheme can still be optimized to correct the chirp along the bunch core. The performance of this scheme will also be better when the non-linear terms in Eq. (2) can be neglected, as these higher order contributions cannot be compensated for in the second plasma stage. Thus, the energy spread of the bunch in the chicane should not exceed the few-percent range, although this condition could be relaxed by including sextupole magnets [46].

Once the chicane R_{56} is determined, the magnet length L_m and bending angle θ experienced by the reference particle can be directly determined from $R_{56} = -2\theta^2(L_d + 2L_m/3)$ [45], where L_d, as defined in Fig. 2, is the length of the drift space between the first and second as well as the third and fourth dipoles. The magnetic field strength can then be obtained as $B = (mc/e)\theta\gamma_{\rm ref}/L_m$. Assuming a bunch with $\chi = E'_z/E_z$ and typical blowout fields, it can be obtained that $R_{56} \simeq 4c/\omega_p \ll 1$ mm for $n_p \gtrsim 10^{16}$ cm^{-3}. Thus, considering $L_m \sim L_d \sim 0.1$ m, the small R_{56} leads to $\theta \ll 0.1$ rad. The high χ characteristic of PBAs therefore allows for a very compact chicane design (~ 1 m) while requiring a very small bending angle. This greatly minimizes the impact of Coherent Synchrotron Radiation (CSR) [47] on the beam parameters.

A possible implementation of this scheme is shown in Fig. 1, where an externally injected electron beam is accelerated by two LWFA stages joined by a magnetic chicane. A combination of active plasma lenses (APLs)

[48] and plasma mirrors [49] could be used for the electron beam transport and laser pulse coupling, respectively, although other configurations are possible. The two laser drivers could originate from splitting a single pulse and thus be intrinsically synchronized.

APLs consist on circular, gas-filled capillaries with $\lesssim$ 1 mm radius, R_c, on which a multi-kV discharge is applied by electrodes at both ends, causing a breakdown of the gas. A current is then driven though the ionized plasma, generating radially symmetric focusing fields with up to kilotesla-per-meter gradients [48]. Although these devices have been observed to suffer from aberrations [48, 50, 51], a solution to this issue has recently been demonstrated [52]. Thanks to the strong and linear focusing fields, APLs are ideal for transporting the highly divergent and high-energy-spread bunches coming out of the first LWFA, as they can be placed sufficiently close to it and thus mitigate the emittance growth in the drift [16]. Futhermore, they show significantly reduced chromaticity with respect to other focusing systems [48]. In practice, APLs could be combined with magnetic quadrupoles to achieve independent control of the focusing in the x and y planes.

The use of plasma mirrors would enable particularly compact setups, as they can be placed close to the laser focus. Tape-based plasma mirrors have already been successfully used for this purpose [53], but they can negatively impact the beam emittance. A promising alternative are liquid crystal films [54], which, due to their nanometer-level thickness, are expected to have negligible impact on the multi-GeV beams considered. Conventional mirrors could also be used, albeit at a cost in compactness, and mirror-less alternatives have also been proposed, such as the use of curved plasma channels [55]. A specific implementation is not considered here.

The presented scheme, apart from offering an energy spread compensation, could also reduce the sensitivity to other critical issues such as the timing jitter between laser driver and witness bunch [56] or the hosing instability [57]. The timing jitter is one of the main challenges of external injection, as it translates into a large energy jitter at the LWFA exit due to the large E_z'. However, thanks to the chicane in this scheme, a temporal injection offset with respect to the ideal phase in the first LWFA would translate, to first order in Eq. (2), into the opposite offset at the second LWFA, thus providing a stable average accelerating field and energy output. Furthermore, since the bunches are accelerated with a large energy chirp, the hosing instability is also mitigated [58, 59].

In order to test the performance of this scheme, start-to-end simulations for a particular set of parameters have been performed. The LWFA stages and APLs have been simulated using the spectral, quasi-3D PIC code FBPIC, while the tracking code ASTRA has been used for the remaining beamline elements taking into account 3D space-charge effects. Additionally, CSRtrack has also been used to account for CSR effects in the chicane.

Motivated by the parameters from the European Plasma Research Accelerator with eXcellence In Applications (known as EuPRAXIA) design study [60], the simulated setup aims at providing 5 GeV electron beams suitable for FEL applications, i.e., a peak current in the kA range, sub-micron emittance and, specially, an energy spread $\lesssim 0.1\%$. For this purpose, we consider an externally injected Gaussian electron bunch with an initial energy of 250 MeV, a 0.5% energy spread with no chirp, a normalized transverse emittance $\epsilon_{n,x} = 0.5$ μm rad, 10 pC of charge, a FWHM duration $\tau = 5$ fs and a peak current $I_{\text{peak}} \simeq 2$ kA. The bunch transverse size, σ_x, is matched [61, 62] to the plasma focusing fields in order to prevent emittance growth. This requires the beam beta function, $\beta_x = \gamma\sigma_x^2/\epsilon_{n,x}$, to satisfy $\beta_x = c/\omega_\beta$ at the LWFA entrance. The normalized emittance is defined as $\epsilon_{n,x} = (\langle x^2\rangle\langle p_x^2\rangle - \langle x p_x\rangle^2)^{1/2}/mc$, where p_x is the transverse particle momentum. Electron beams within this range of parameters can be produced with conventional accelerators [63–65], and diagnostics for these ultra-short bunches are under active development [66]. The two identical LWFAs have a length $L_p = 8$ cm and a parabolic transverse density profile for laser pulse guiding $n_p = n_{p,0} + r^2/\pi r_e w_0^4$, where $n_{p,0} = 10^{17}$ cm^{-3} is the on-axis plasma density, r the radial coordinate, r_e the classical electron radius and w_0 the spot size of the laser driver. Plasma cells in this range of parameters have been recently demonstrated [67, 68]. For simplicity, a longitudinal flat-top plasma density profile has been considered, although the presence of smooth plasma-to-vacuum transitions would be beneficial for electron beam matching [69] and emittance growth minimization [70]. This choice of electron beam and plasma parameters also helps in reducing below the 10^{-4} level the relative energy spread generated in the LWFAs due to slice mixing from betatron motion [71]. Each LWFA is driven by a 40 J, 0.75 PW laser pulse with a peak normalized vector potential $a_0 = 3$, a spot size $w_0 = 50$ μm and a FWHM duration $\tau_0 = 50$ fs. This laser can be successfully guided throughout the LWFAs, which provide an energy gain of ~ 2.6 GeV each. The APLs are placed 3 cm away from the LWFAs and provide a focusing gradient of 3 kT/m, as demonstrated experimentally [48]. They have a length of 6.6 cm, optimized to achieve a beam waist at the chicane center, and a plasma density $n_p^{\text{APL}} = 10^{15}$ cm^{-3}, which was chosen in order to minimize the impact of beam-driven wakefields [72]. The chicane has a total length of 1.2 m, with $L_d = 12.5$ cm and dipoles with $L_m = 20$ cm and $B = 0.54$ T for a bending angle of $\theta = 0.011$ rad.

An overview of the simulation results can be seen in Fig. 3. The electron bunch leaves the first LWFA with preserved emittance, an energy of ~ 2.9 GeV and a chirp $\chi \simeq -0.031$ μm^{-1} (equivalent to ~ 90 MeV/μm in absolute units), which induces a total relative energy spread $\sim 2\%$. As a consequence, the projected emittance grows

after the accelerating stage until the beam divergence is controlled by the APL, where the maximum beam size is $\sigma_r \simeq 15\ \mu\text{m} \ll R_c$. ASTRA and CSRtrack simulations show that the influence of space-charge and CSR on the beam parameters is negligible thanks to its GeV energy and the small bending angle. The beam is then focused by the following APL and injected into the second LWFA, where it gains an additional ~ 2.6 GeV for a final energy of ~ 5.5 GeV while compensating the energy chirp.

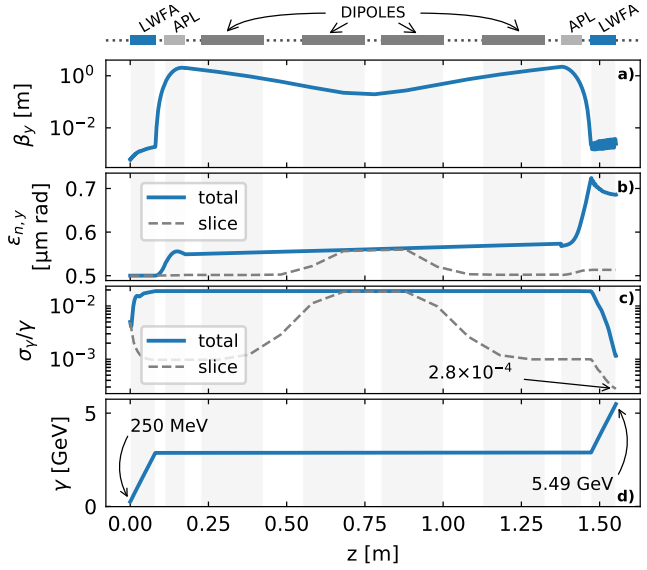

FIG. 3. Evolution of beam parameters along the accelerator: (a) beta function, (b) normalized emittance, (c) energy spread, and (d) energy. Transverse parameters are shown for the y plane, which is not affected by dispersion in the chicane. Final values in x and y planes are virtually identical (difference of $\ll 1\%$). Slice parameters grow in the chicane center due to shorter bunch duration because the slice length (0.1 μm) is kept constant.

As seen in Fig. 4, the total energy spread has been reduced by a factor of ~ 20 down to 0.12% with respect to a case with no chirp compensation. This corresponds to a dechirping strength of 1.1 GeV/μm/m, orders of magnitude higher than in other schemes [34–38]. The slice energy spread has also been reduced to just 2.8×10^{-4}, when considering 0.1 μm slices. These values are at least one order of magnitude below state-of-art LWFAs and would satisfy the requirements for an X-ray FEL [23]. The discrepancy between the total and slice energy spread arises from second order contributions in the chicane, which induce the slight parabolic bunch shape seen in Fig. 4b.

The emittance evolution in the drifts and APLs is well controlled, achieving a final value of 0.69 μm rad (total) and 0.51 μm rad (slice). The projected emittance growth arises from the large energy chirp along the bunch, which causes individual slices to diverge (or converge) at different rates in the drifts and to have a different betatron frequency in the APLs. However, it should be noted that this growth is not the same in both APLs, but it is more moderate in the first one. This is due to the beam-induced focusing wakefields, which, for a short bunch, grow linearly towards the tail [72] and, for a case with $\chi < 0$, can mitigate the projected emittance growth by equalizing ω_β along the bunch. This suggests that wakefields in APLs, which are typically regarded as a key limitation of these devices [72], can also be useful and could be optimized for emittance preservation in bunches with a large negative energy chirp. Another consequence of this slice decoherence is that the beta function will evolve differently along the bunch. Therefore, not all slices will be matched to the focusing fields in the second LWFA, causing the oscillations seen in Fig. 3a.

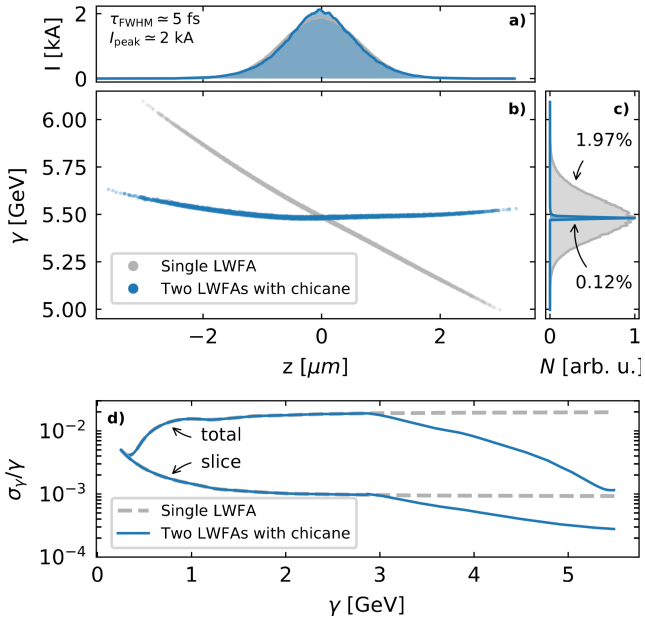

FIG. 4. Comparison of the final bunch properties with respect to a case with acceleration in a single LWFA (same driver and plasma profile but ~ 20 cm long). The bunch current (a), longitudinal phase space (b) and energy profile (c) normalized to the peak number of counts, N, are shown. The energy spread evolution during acceleration can be seen in (d).

The presented scheme therefore offers a path towards beams with ultra-low energy spread ($\sim 10^{-4}$) while reducing the sensitivity to issues such as the timing jitter for external injection and the hosing instability. The dechirping strength offered by this concept is orders of magnitude higher than in other proposals [34–38], and allows for dechirping while further accelerating the beam. The concept is ideally suited for PBAs with weakly or linearly beam-loaded wakefields where the beam develops a negative chirp before the magnetic chicane. Electron beams obtained with this multistage setup would enable ground breaking applications, such as compact FELs. Furthermore, this setup could be scaled to higher energies thanks to its modular design, potentially en-

abling other applications such as plasma-based colliders. This could be achieved either by introducing additional plasma stages while keeping a single central chicane, or by repeating multiple sections of one chicane every two plasma accelerating modules.

This project has received funding from the European Union's Horizon 2020 research and innovation programme under grant agreement No. 653782. We acknowledge the use of the High-Performance Cluster (Maxwell) at DESY for the numerical simulations. We would like to thank T. Mehrling, S.K. Barber, S. Steinke, M. Dohlus and K. Floetmann for useful discussions.

* angel.ferran.pousa@desy.de

[1] P. Chen, J. M. Dawson, R. W. Huff, and T. Katsouleas, Phys. Rev. Lett. **54**, 693 (1985).
[2] T. Tajima and J. M. Dawson, Phys. Rev. Lett. **43**, 267 (1979).
[3] J. Faure, C. Rechatin, A. Norlin, A. Lifschitz, Y. Glinec, and V. Malka, Nature (London) **444**, 737 (2006).
[4] V. Malka, J. Faure, Y. A. Gauduel, E. Lefebvre, A. Rousse, and K. T. Phuoc, Nat. Phys. **4**, 447 (2008).
[5] W. P. Leemans, B. Nagler, A. J. Gonsalves, C. Tóth, K. Nakamura, C. G. Geddes, E. Esarey, C. Schroeder, and S. Hooker, Nat. Phys. **2**, 696 (2006).
[6] X. Wang, R. Zgadzaj, N. Fazel, Z. Li, S. Yi, X. Zhang, W. Henderson, Y.-Y. Chang, R. Korzekwa, H.-E. Tsai, *et al.*, Nat. Comm. **4**, 1988 (2013).
[7] W. Leemans, A. Gonsalves, H.-S. Mao, K. Nakamura, C. Benedetti, C. Schroeder, C. Tóth, J. Daniels, D. Mittelberger, S. Bulanov, *et al.*, Phys. Rev. Lett. **113**, 245002 (2014).
[8] M. Mirzaie, S. Li, M. Zeng, N. Hafz, M. Chen, G. Li, Q. Zhu, H. Liao, T. Sokollik, F. Liu, *et al.*, Sci. Rep. **5**, 14659 (2015).
[9] A. J. Gonsalves, K. Nakamura, J. Daniels, C. Benedetti, C. Pieronek, T. C. H. de Raadt, S. Steinke, J. H. Bin, S. S. Bulanov, J. van Tilborg, C. G. R. Geddes, C. B. Schroeder, C. Tóth, E. Esarey, K. Swanson, L. Fan-Chiang, G. Bagdasarov, N. Bobrova, V. Gasilov, G. Korn, P. Sasorov, and W. P. Leemans, Phys. Rev. Lett. **122**, 084801 (2019).
[10] S. Fritzler, E. Lefebvre, V. Malka, F. Burgy, A. E. Dangor, K. Krushelnick, S. P. D. Mangles, Z. Najmudin, J.-P. Rousseau, and B. Walton, Phys. Rev. Lett. **92**, 165006 (2004).
[11] E. Brunetti, R. Shanks, G. Manahan, M. Islam, B. Ersfeld, M. Anania, S. Cipiccia, R. Issac, G. Raj, G. Vieux, *et al.*, Phys. Rev. Lett. **105**, 215007 (2010).
[12] O. Lundh *et al.*, Nat. Phys. **7**, 219 (2011).
[13] J. Couperus, R. Pausch, A. Köhler, O. Zarini, J. Krämer, M. Garten, A. Huebl, R. Gebhardt, U. Helbig, S. Bock, *et al.*, Nat. Comm. **8**, 487 (2017).
[14] A. Ferran Pousa, R. Assmann, and A. M. de la Ossa, in *9th Int. Particle Accelerator Conf.(IPAC'18)*, edited by S. Koscielniak, T. Satogata, V. R. Schaa, and J. Thomson (JACOW Publishing, Geneva, Switzerland, 2018) pp. 607–611.
[15] K. Floettmann, Phys. Rev. ST Accel. Beams **6**, 034202 (2003).
[16] M. Migliorati, A. Bacci, C. Benedetti, E. Chiadroni, M. Ferrario, A. Mostacci, L. Palumbo, A. R. Rossi, L. Serafini, and P. Antici, Phys. Rev. ST Accel. Beams **16**, 011302 (2013).
[17] C. B. Schroeder, E. Esarey, C. G. R. Geddes, C. Benedetti, and W. P. Leemans, Phys. Rev. ST Accel. Beams **13**, 101301 (2010).
[18] F. Grüner, S. Becker, U. Schramm, T. Eichner, M. Fuchs, R. Weingartner, D. Habs, J. Meyer-ter Vehn, M. Geissler, M. Ferrario, L. Serafini, B. van der Geer, H. Backe, W. Lauth, and S. Reiche, Appl. Phys. B **86**, 431 (2007).
[19] M. Fuchs, R. Weingartner, A. Popp, Z. Major, S. Becker, J. Osterhoff, I. Cortrie, B. Zeitler, R. Hörlein, G. D. Tsakiris, U. Schramm, T. P. Rowlands-Rees, S. M. Hooker, D. Habs, F. Krausz, S. Karsch, and F. Grüner, Nat. Phys. **5**, 826 (2009).
[20] A. R. Maier, A. Meseck, S. Reiche, C. B. Schroeder, T. Seggebrock, and F. Gruner, Phys. Rev. X **2**, 031019 (2012).
[21] Z. Huang, Y. Ding, and C. B. Schroeder, Phys. Rev. Lett. **109**, 204801 (2012).
[22] A. Loulergue, M. Labat, C. Evain, C. Benabderrahmane, V. Malka, and M. E. Couprie, New Journal of Physics **17**, 023028 (2015).
[23] S. Corde, K. T. Phuoc, G. Lambert, R. Fitour, V. Malka, A. Rousse, A. Beck, and E. Lefebvre, Rev. Mod. Phys **85**, 1 (2013).
[24] S. Wilks, T. Katsouleas, J. M. Dawson, and J. J. Su, Part. Accel. **22**, 81 (1987).
[25] K. V. Lotov, Phys. Plasmas **12**, 053105 (2005).
[26] M. Tzoufras, W. Lu, F. S. Tsung, C. Huang, W. B. Mori, T. Katsouleas, J. Vieira, R. A. Fonseca, and L. O. Silva, Phys. Rev. Lett. **101**, 145002 (2008).
[27] S. Y. Kalmykov, A. Beck, S. A. Yi, V. N. Khudik, M. C. Downer, E. Lefebvre, B. A. Shadwick, and D. P. Umstadter, Phys. Plasmas **18**, 056704 (2011).
[28] E. Esarey, C. Schroeder, and W. Leemans, Rev. Mod. Phys. **81**, 1229 (2009).
[29] C. B. Schroeder, C. Benedetti, E. Esarey, and W. P. Leemans, Phys. Rev. Lett. **106**, 135002 (2011).
[30] R. Brinkmann, N. Delbos, I. Dornmair, M. Kirchen, R. Assmann, C. Behrens, K. Floettmann, J. Grebenyuk, M. Gross, S. Jalas, T. Mehrling, A. Martinez de la Ossa, J. Osterhoff, B. Schmidt, V. Wacker, and A. R. Maier, Phys. Rev. Lett. **118**, 214801 (2017).
[31] A. Döpp, C. Thaury, E. Guillaume, F. Massimo, A. Lifschitz, I. Andriyash, J.-P. Goddet, A. Tazfi, K. Ta Phuoc, and V. Malka, Phys. Rev. Lett. **121**, 074802 (2018).
[32] G. Manahan, A. Habib, P. Scherkl, P. Delinikolas, A. Beaton, A. Knetsch, O. Karger, G. Wittig, T. Heinemann, Z. Sheng, *et al.*, Nat. Comm. **8** (2017).
[33] Y. P. Wu, J. F. Hua, C. H. Pai, X. L. Xu, C. J. Zhang, F. Li, Y. Wan, Z. Nie, W. Lu, W. B. Mori, and C. Joshi, arXiv preprint arXiv:1805.07031 (2018).
[34] K. Bane and G. Stupakov, Nucl. Instr. Meth. Phys. Res., Sect. A **690**, 106 (2012).
[35] S. Antipov, S. Baturin, C. Jing, M. Fedurin, A. Kanareykin, C. Swinson, P. Schoessow, W. Gai, and A. Zholents, Phys. Rev. Lett. **112**, 114801 (2014).
[36] R. D'Arcy, S. Wesch, A. Aschikhin, S. Bohlen, C. Behrens, M. J. Garland, L. Goldberg, P. Gonzalez, A. Knetsch, V. Libov, A. M. de la Ossa, M. Meisel, T. J. Mehrling, P. Niknejadi, K. Poder, J.-H. Röckemann,

L. Schaper, B. Schmidt, S. Schröder, C. Palmer, J.-P. Schwinkendorf, B. Sheeran, M. J. V. Streeter, G. Tauscher, V. Wacker, and J. Osterhoff, Phys. Rev. Lett. **122**, 034801 (2019).
[37] V. Shpakov, M. P. Anania, M. Bellaveglia, A. Biagioni, F. Bisesto, F. Cardelli, M. Cesarini, E. Chiadroni, A. Cianchi, G. Costa, M. Croia, A. Del Dotto, D. Di Giovenale, M. Diomede, M. Ferrario, F. Filippi, A. Giribono, V. Lollo, M. Marongiu, V. Martinelli, A. Mostacci, L. Piersanti, G. Di Pirro, R. Pompili, S. Romeo, J. Scifo, C. Vaccarezza, F. Villa, and A. Zigler, Phys. Rev. Lett. **122**, 114801 (2019).
[38] Y. P. Wu, J. F. Hua, Z. Zhou, J. Zhang, S. Liu, B. Peng, Y. Fang, Z. Nie, X. N. Ning, C.-H. Pai, Y. C. Du, W. Lu, C. J. Zhang, W. B. Mori, and C. Joshi, Phys. Rev. Lett. **122**, 204804 (2019).
[39] R. Lehe, M. Kirchen, I. A. Andriyash, B. B. Godfrey, and J.-L. Vay, Comput. Phys. Commun. **203**, 66 (2016).
[40] K. Floettmann, Manual, Version (2017).
[41] M. Dohlus, A. Kabel, and T. Limberg, Nucl. Instr. Meth. Phys. Res., Sect. A **445**, 338 (2000).
[42] J. B. Rosenzweig, B. Breizman, T. Katsouleas, and J. J. Su, Phys. Rev. A **44**, R6189 (1991).
[43] K. Lotov, Phys. Rev. E **69**, 046405 (2004).
[44] W. Lu, C. Huang, M. Zhou, W. B. Mori, and T. Katsouleas, Phys. Rev. Lett. **96**, 165002 (2006).
[45] A. W. Chao, K. H. Mess, M. Tigner, and F. Zimmermann, *Handbook of accelerator physics and engineering* (World Scientific, 1999).
[46] R. J. England, J. B. Rosenzweig, G. Andonian, P. Musumeci, G. Travish, and R. Yoder, Phys. Rev. ST Accel. Beams **8**, 012801 (2005).
[47] M. Dohlus and T. Limberg, Nucl. Instr. Meth. Phys. Res., Sect. A **393**, 494 (1997), free Electron Lasers 1996.
[48] J. van Tilborg, S. Steinke, C. G. R. Geddes, N. H. Matlis, B. H. Shaw, A. J. Gonsalves, J. V. Huijts, K. Nakamura, J. Daniels, C. B. Schroeder, C. Benedetti, E. Esarey, S. S. Bulanov, N. A. Bobrova, P. V. Sasorov, and W. P. Leemans, Phys. Rev. Lett. **115**, 184802 (2015).
[49] C. Thaury, F. Quéré, J.-P. Geindre, A. Levy, T. Ceccotti, P. Monot, M. Bougeard, F. Réau, P. d'Oliveira, P. Audebert, *et al.*, Nat. Phys. **3**, 424 (2007).
[50] R. Pompili, M. P. Anania, M. Bellaveglia, A. Biagioni, S. Bini, F. Bisesto, E. Brentegani, G. Castorina, E. Chiadroni, A. Cianchi, M. Croia, D. Di Giovenale, M. Ferrario, F. Filippi, A. Giribono, V. Lollo, A. Marocchino, M. Marongiu, A. Mostacci, G. Di Pirro, S. Romeo, A. R. Rossi, J. Scifo, V. Shpakov, C. Vaccarezza, F. Villa, and A. Zigler, Appl. Phys. Lett. **110**, 104101 (2017).
[51] J. van Tilborg, S. K. Barber, C. Benedetti, C. B. Schroeder, F. Isono, H.-E. Tsai, C. G. R. Geddes, and W. P. Leemans, Phys. Plasmas **25**, 056702 (2018).
[52] C. A. Lindstrøm, E. Adli, G. Boyle, R. Corsini, A. E. Dyson, W. Farabolini, S. M. Hooker, M. Meisel, J. Osterhoff, J.-H. Röckemann, L. Schaper, and K. N. Sjobak, Phys. Rev. Lett. **121**, 194801 (2018).
[53] S. Steinke, J. Van Tilborg, C. Benedetti, C. Geddes, C. Schroeder, J. Daniels, K. Swanson, A. Gonsalves, K. Nakamura, N. Matlis, *et al.*, Nature **530**, 190 (2016).
[54] P. Poole, A. Krygier, G. Cochran, P. Foster, G. Scott, L. Wilson, J. Bailey, N. Bourgeois, C. Hernandez-Gomez, D. Neely, *et al.*, Sci. Rep. **6**, 32041 (2016).
[55] J. Luo, M. Chen, W. Y. Wu, S. M. Weng, Z. M. Sheng, C. B. Schroeder, D. A. Jaroszynski, E. Esarey, W. P. Leemans, W. B. Mori, and J. Zhang, Phys. Rev. Lett. **120**, 154801 (2018).
[56] A. Ferran Pousa, R. W. Assmann, R. Brinkmann, and A. Martinez de la Ossa, J. Phys.: Conf. Ser. **874**, 012032 (2017).
[57] D. H. Whittum, W. M. Sharp, S. S. Yu, M. Lampe, and G. Joyce, Phys. Rev. Lett. **67**, 991 (1991).
[58] R. Lehe, C. B. Schroeder, J.-L. Vay, E. Esarey, and W. P. Leemans, Phys. Rev. Lett. **119**, 244801 (2017).
[59] T. J. Mehrling, R. A. Fonseca, A. Martinez de la Ossa, and J. Vieira, Phys. Rev. Lett. **118**, 174801 (2017).
[60] P. A. Walker *et al.*, J. Phys.: Conf. Ser. **874**, 012029 (2017).
[61] R. Assmann and K. Yokoya, Nucl. Instr. Meth. Phys. Res., Sect. A **410**, 544 (1998).
[62] T. Mehrling, J. Grebenyuk, F. S. Tsung, K. Floettmann, and J. Osterhoff, Phys. Rev. ST Accel. Beams **15**, 111303 (2012).
[63] J. Zhu, R. Aßmann, A. Ferran Pousa, B. Marchetti, and P. A. Walker, in *9th Int. Particle Accelerator Conf.(IPAC'18)*, edited by S. Koscielniak, T. Satogata, V. R. Schaa, and J. Thomson (JACOW Publishing, Geneva, Switzerland, 2018) pp. 3025–3028.
[64] B. Marchetti, R. Assmann, U. Dorda, and J. Zhu, Appl. Sci. **8** (2018).
[65] J. Zhu, R. W. Assmann, M. Dohlus, U. Dorda, and B. Marchetti, Phys. Rev. Accel. Beams **19**, 054401 (2016).
[66] P. Craievich, R. Aßmann, M. Bopp, H.-H. Braun, N. Catalan Lasheras, F. Christie, R. D'Arcy, U. Dorda, M. Foese, R. Ganter, P. Gonzalez Caminal, A. Grudiev, M. Hoffmann, M. Hüning, R. Jonas, T. Kleeb, O. Krebs, S. Lederer, V. Libov, B. Marchetti, D. Marx, G. McMonagle, J. Osterhoff, M. Pedrozzi, F. Poblotzki, E. Prat, S. Reiche, M. Reukauff, H. Schlarb, S. Schreiber, G. Tews, M. Vogt, A. d. Z. Wagner, W. Wuensch, and R. Zennaro, in *9th Int. Particle Accelerator Conf.(IPAC'18)*, edited by S. Koscielniak, T. Satogata, V. R. Schaa, and J. Thomson (JACoW Publishing, Geneva, Switzerland, 2018) pp. 3808–3811.
[67] R. J. Shalloo, C. Arran, L. Corner, J. Holloway, J. Jonnerby, R. Walczak, H. M. Milchberg, and S. M. Hooker, Phys. Rev. E **97**, 053203 (2018).
[68] R. J. Shalloo, C. Arran, A. Picksley, A. von Boetticher, L. Corner, J. Holloway, G. Hine, J. Jonnerby, H. M. Milchberg, C. Thornton, R. Walczak, and S. M. Hooker, Phys. Rev. Accel. Beams **22**, 041302 (2019).
[69] K. Floettmann, Phys. Rev. ST Accel. Beams **17**, 054402 (2014).
[70] I. Dornmair, K. Floettmann, and A. R. Maier, Phys. Rev. ST Accel. Beams **18**, 041302 (2015).
[71] A. Ferran Pousa, R. Assmann, and A. Martinez de la Ossa, arXiv preprint arXiv:1804.10966 (2018).
[72] C. A. Lindstrøm and E. Adli, arXiv preprint arXiv:1802.02750 (2018).